

## 199. The Solid-State and Solution Conformations of (+)-Chelidonine

by Miyoko Kamiguchi\*, Yuko Miyamoto, Kinuko Iwasa, Makiko Sugiura, Zjujiro Nishijo, and Narao Takao

Kobe Women's College of Pharmacy, 4-19-1, Motoyamakitamachi, Higashinada-ku, Kobe 658, Japan

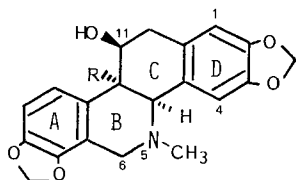
and Toshimasa Ishida, Yasuko In, and Masatoshi Inoue

Osaka University of Pharmaceutical Sciences, 2-10-65, Kawai, Matsubara 580, Japan

(6. VII. 90)

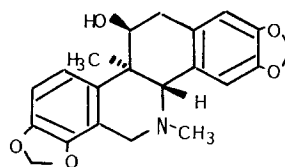
The solid-state and solution conformations of (+)-chelidonine (**1**), a biologically active alkaloid, were determined by X-ray diffraction and  $^1\text{H-NMR}$  spectroscopy. X-Ray diffraction analysis revealed a conformer with B/C 'anti-type' *cis* conjunction, a half-chair of ring B, and a twist half-chair of ring C. One  $\text{H}_2\text{O}$  molecule per one alkaloid molecule was cocrystallized and stabilized by H-bonding with  $\text{OH}-\text{C}(11)$ . Analysis of the thermal behavior of the crystal showed more thermal stability in the monohydrate than the anhydrate. The NMR measurement of concentration and temperature dependences in  $\text{CDCl}_3$  and in  $(\text{CD}_3)_2\text{SO}$  suggested that the OH group of **1** was intramolecularly H-bonded to N(5) in  $(\text{CD}_3)_2\text{SO}$  and intermolecularly H-bonded to the solvent in  $\text{CDCl}_3$ . Conformational-energy calculations by the MNDO method showed that the intramolecular H-bond was little affected by the conformational stabilization of **1**.

**Introduction.** – (+)-Chelidonine (**1**), a biologically active alkaloid, was first isolated from *Chelidonium majus* (Papaveraceae) in 1839 [1]. Extensive chemical and spectroscopic studies [2] [3] led to its correct attribution to the hydrobenzo[*c*]phenanthridine-type alkaloid class [4].



**1** R = H (+)-chelidonine

**2** R =  $\text{CH}_3$  (+)-corynoline



**3** (+)-14-epicorynoline

The solution conformation of **1**, including its absolute configuration, has been established by IR-,  $^1\text{H}$ - and  $^{13}\text{C-NMR}$ -, and CD-spectroscopic methods [5–8]. On the other hand, although the alkaloid in the solid state has shown several crystal forms depending on the solvents [4], little attention has been paid to this aspect. We believe that the conformational study of **1** in the solid state and the energetical study of its conformation will provide basic information about the pharmacological properties of hydrobenzo[*c*]phenanthridine-type alkaloids [4] [9]. The presence of an intramolecular H-bond between N(5) and OH was detected by IR spectroscopy in 1958 [3]. However, the IR spectrum

alone is considered insufficient to establish a conformation involving the orientation of the OH group of **1** in  $\text{CHCl}_3$ .

The aim of the present study was to determine by X-ray analysis the crystal structure of **1**, to examine the thermal behavior of **1** in the crystalline state, to study in detail the  $^1\text{H-NMR}$  behavior of **1** in  $\text{CDCl}_3$  in order to ascertain the intramolecular H-bond between N(5) and OH, and to estimate by the MNDO method the energetic preference between two conformers with and without an intramolecular H-bond.

**Results and Discussion.** – *Molecular Structure of (+)-Chelidionine (1)*. The projection on the ring-D plane of the (+)-chelidionine (**1**) structure obtained by X-ray crystal analysis is presented in Fig. 1. Atom coordinates and thermal parameters and bond lengths and angles with their standard deviations have been deposited with the *Cambridge Crystallographic Data Center*. All bond lengths and angles are normal and within the range found in the crystal structures of hydrobenzo[*c*]phenanthridine-type alkaloids such as ( $\pm$ )-corynoline (**2**) [10] (+)-14-epicorynoline (**3**) bromoacetate [11], and (+)-chelidionine 4-bromobenzoate [12].

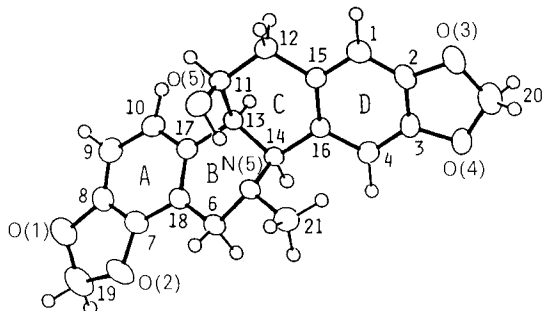


Fig. 1. View of the molecular structure of **1** and numbering (partially arbitrary)

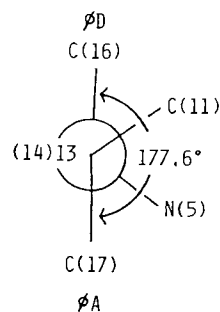


Fig. 2. Torsion angles [°] about the C(13)–C(14) bond of **1**

The molecular conformation of **1** has an 'anti-cis' form [12] with respect to the *cis*-fused B/C moiety (Fig. 2). The dihedral angle between the mean planes of ring A and ring D is  $47.80^\circ$ , and the angle C(17)–C(13)–C(14)–C(16) between the two rings in the *Newman* projection is  $177.6^\circ$  (Fig. 2). These values are similar to those for **2** [10], *i.e.*  $46.79$  and  $173.6^\circ$ , respectively, leading to the supposition that they are typical conformational data for an 'anti-cis' conformation of the B/C-*cis*-fused hydrobenzo[*c*]phenanthridine alkaloids. Ring B is in a half-chair conformation and ring C in a twist half-chair conformation (Fig. 3). The conformation of ring C of **1** is also similar to that of **2**. Inspection of a *Dreiding* model reveals that this twisted conformation relaxes the steric hindrance caused by the 1,3-diaxial interaction of the bonds C(14)–N(5)/C(11)–O(5) and H–C(12)/H–C(13) and by *van der Waals* repulsion between the H-atoms of the  $\text{CH}_3\text{N}$  group and H–C(4). Therefore, such a twisted half-chair conformation of ring C must be intrinsic and is a stable conformation for the hydrobenzo[*c*]phenanthridine-type alkaloids. The torsion angles H(11)–C(11)–C(12)–H(12A) and H(11)–C(11)–C(12)–H(12B) obtained from the X-ray structure of **1** are in agreement with those obtained from the  $^1\text{H-NMR}$  measurements ( $81.3(5)$  and  $36.4(5)$ , resp., *vs.*  $90$  and  $30^\circ$ , resp. [6]).

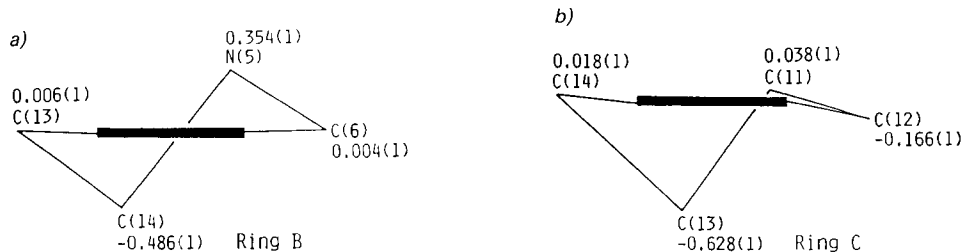


Fig. 3. Schematic projection of rings B and C of **1**, with deviations [Å] of atoms from the least-square plane of the neighbouring aromatic ring (e.s.d.'s in parentheses). The bold-face bar stands for the aromatic ring, i.e. ring A in a) and ring D in b).

The solid-state structure of **1** shows an axial O(5)H–C(11) and an equatorial CH<sub>3</sub>–N group (see Fig. 1). Since the N(5)···O(5) distance is 2.69 Å, the interaction force of the intramolecular H-bond would be somewhat stronger than in **2** (2.79 Å) [10]. A remarkable feature of the solid state of **1** is the presence of an H<sub>2</sub>O molecule located in the neighborhood of O(5).

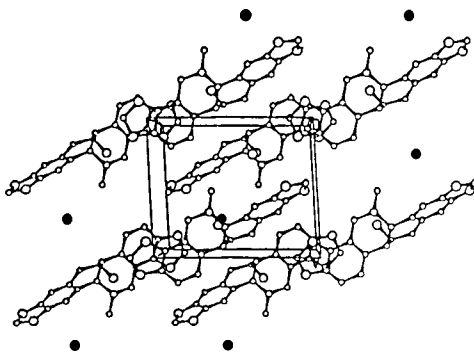


Fig. 4. Crystal packing of **1**, viewed along the *b* axis. H<sub>2</sub>O molecules are represented by filled circles.

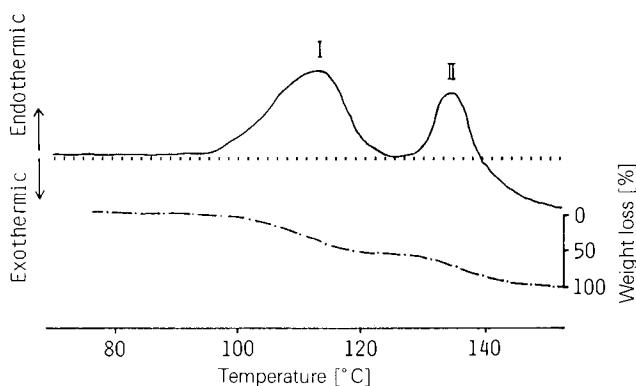
Crystal packing as viewed along the *b* axis is shown in Fig. 4. Ring A involving methylenedioxy moieties is located on the diad screw axis of the crystal lattice and piles up along the *b* axis, thus forming infinite stacking layers. The molecules are stably held by *van der Waals* interactions and H-bonds for which the distances are given in Table 1.

*Thermal Behavior of 1 in the Crystalline State.* The thermal behavior of a crystal of **1** was studied using a DTA-TG profile corresponding to an increase in temperature. Fig. 5 shows the result. Peak I represents an endothermic change accompanying the release of a crystallized H<sub>2</sub>O molecule ( $T_{\max}$  113°), and peak II reveals another endothermic change corresponding to the melting point ( $T_{\max}$  136°); finally, the crystal decomposes. The release temperature for H<sub>2</sub>O from the crystal is relatively high, just below the melting and decomposition temperature. This strongly suggests that in the crystal structure of **1**, H<sub>2</sub>O forms an energetically favorable H-bond with O(5).

*NMR Measurements.* Although the <sup>1</sup>H-NMR assignments of **1** in CDCl<sub>3</sub> have been reported by several authors [5–7], the behavior of the OH group has been unexplored. We

Table 1. Intermolecular Short Contacts [Å] for **1**

Atom 1	Atom 2	Distance	Symmetry operation
O(1w)	O(1)	3.209 (5)	$x - 1, y, z - 1$
N(5)	O(5)	2.702 (4)	$x, y, z$
O(2)	C(1)	3.315 (5)	$x, y, z + 1$
O(2)	C(2)	3.181 (5)	$x, y, z + 1$
O(2)	O(3)	3.337 (4)	$x, y, z + 1$
O(1)	C(20)	3.363 (6)	$x + 1, y, z + 1$
N(5)	O(4)	3.345 (4)	$-x + 1, y - 0.50, -z + 1$
O(5)	O(4)	3.210 (4)	$-x + 1, y - 0.50, -z + 1$
O(5)	O(1w)	2.763 (5)	$-x + 1, y - 0.50, -z + 1$
O(4)	N(5)	3.384 (4)	$-x + 1, y + 0.50, -z + 1$
O(1w)	O(5)	2.773 (5)	$-x + 1, y + 0.50, -z + 1$
O(5)	C(19)	3.356 (6)	$-x + 2, y - 0.50, -z + 2$
O(4)	C(9)	3.457 (5)	$-x + 2, y, + 0.50, -z + 1$

Fig. 5. DTA-TG profile of crystalline (+)-chelidonine (**1**)

believe that distinguishing the intra- or intermolecularly H-bonded OH proton of **1** from the solvent-exposed one will provide basic information on the energetically stable conformation of B/C-*cis* fused hydrobenzo[*c*]phenanthridine alkaloids in solution.

The temperature dependence of the CONH chemical shift in various solvents has been used to distinguish between 'exposed' and 'buried' NH groups of peptides [13]. In a similar manner, the OH protons of **1** and **2** have now been investigated. The temperature dependences of the OH chemical shifts of **1** and **2** in  $(\text{CD}_3)_2\text{SO}$  and  $\text{CDCl}_3$  were measured between 25 and 55°, with increments of 5°, and the temperature coefficient ( $d\delta/dT$  [ppm/°]), as calculated from the least-squares equation, are given in Fig. 6a. The line profiles can be classified into two types of behaviour. In  $(\text{CD}_3)_2\text{SO}$  solution, the OH proton of **1** shows a significantly low temperature coefficient ( $d\delta/dT = -0.3 \cdot 10^{-3}$  ppm/°), although the remaining protons fall within values of  $-5 \cdot 10^{-3}$  to  $-7 \cdot 10^{-3}$  ppm/°. This suggests that in  $(\text{CD}_3)_2\text{SO}$  solution, the molecular state in which the OH proton is involved in an intramolecular H-bond (and thus forms a solvent-shielded environment) is predominant. On the other hand, it is also possible that the OH proton of **1** and **2** in  $\text{CDCl}_3$ , as well as of **2** in  $(\text{CD}_3)_2\text{SO}$  participates in the interaction with the solvent.

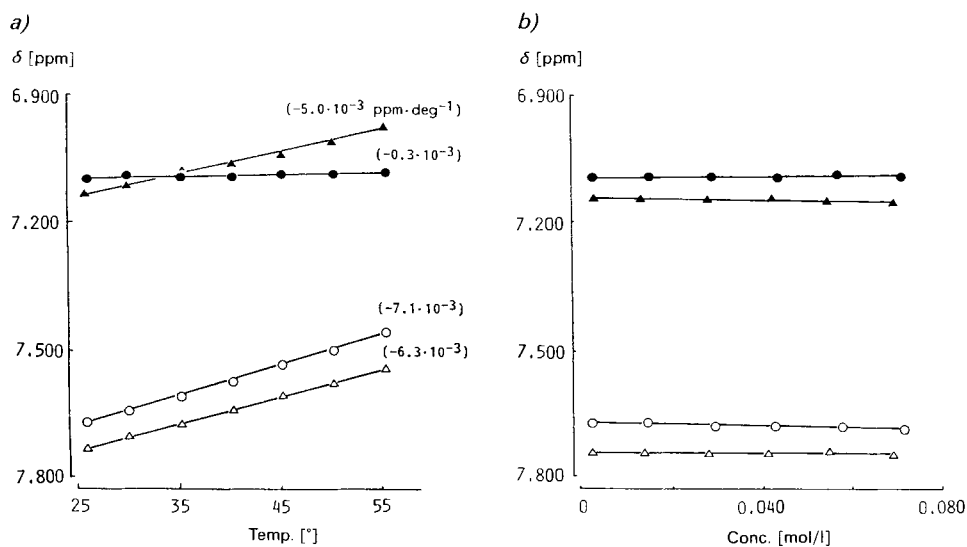


Fig. 6. a) Temperature Dependences and b) Concentration Dependences of Chemical Shifts of the OH Protons of **1** and **2**. **1** in  $(\text{CD}_3)_2\text{SO}$  (●) and in  $\text{CDCl}_3$  (○); **2** in  $(\text{CD}_3)_2\text{SO}$  (▲) and in  $\text{CDCl}_3$  (△).

The concentration dependence of the chemical shift of the OH proton of **1** and **2** was measured at room temperature in the range of 3–72 mM in  $(\text{CD}_3)_2\text{SO}$  and  $\text{CDCl}_3$  solutions (Fig. 6b): the chemical shifts remain practically unchanged. This precludes the possibility of an intermolecular interaction, suggesting that the molecules present in solution behave independently. Therefore, the above mentioned straight-line plot of  $\delta$  values of **1** in  $(\text{CD}_3)_2\text{SO}$  vs. temperature ( $d\delta/dT = -0.3 \cdot 10^{-3} \text{ ppm}/^\circ$ ) reflects the behaviour of an 'independent' molecule, and the conformation with an intramolecular H-bond could be proposed as the preferred form of this molecule in  $(\text{CD}_3)_2\text{SO}$  solution.

With the exception of the OH proton, all chemical shifts and coupling constants of **1** and **2** remain practically unchanged in the observed temperature and concentration ranges, and the values are essentially the same as those reported previously [6] [7].

**Conformational-Energy Values.** Although the X-ray studies suggested that the conformations of **1** and **2** are both 'anti-cis' and stabilized by an intramolecular H-bond, a difference can be observed in the NMR behavior of their OH proton (see above). In order to make the participation of the OH group in the intramolecular H-bond more clear, the energetic stability of the possibly involved conformers was examined by modified neglect of diatomic overlap (MNDO) calculations.

Table 2. Conformational-Energy Values for **1** and **2**, Obtained from MNDO Calculations

	Total energy $E$ [kcal/mol]		$ E(\mathbf{A}) - E(\mathbf{B}) $ [kcal/mol]	Preferred conformer	Ref.
	Conformer A, with H-bond	Conformer B, without H-bond			
<b>1</b>	-106970.98	-107005.08	34.10	<b>B</b>	This work
<b>2</b>	-110463.28	-110459.69	3.59	<b>A</b>	[10]

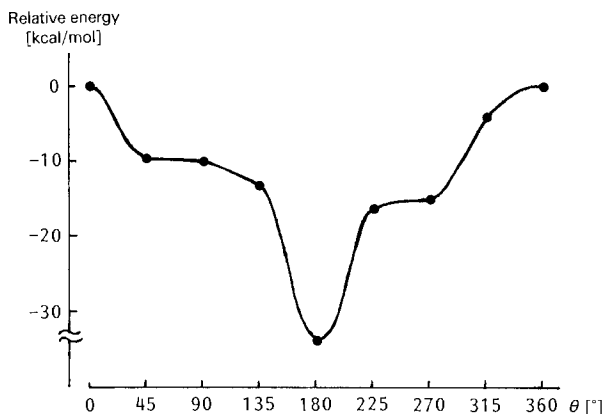


Fig. 7. Energy variation of **1** as a function of the rotation of the OH–C(11) bond. The torsion angle ( $\theta$ ) of C(13)–C(11)–O(5)–H(5O) was rotated from 0 to 360° at intervals of 45°.

Table 2 shows the total-energy values  $E$  for the conformers with (A) or without an intramolecular H-bond (B) of **1** and **2**. In the case of **2**, conformer A was energetically more stable than conformer B by 3.59 kcal/mol, which corresponds to a H-bonding energy. In contrast, for **1**, conformer B was more stable than A, the energy difference being 34.1 kcal/mol. However, this difference seems to be much too large when compared with the values usually expected. Therefore, in order to examine the reasonability of the calculation, the energy change accompanying rotation of the OH–C(11) bond was analysed, and the energy profile obtained is shown in Fig. 7. The profile shows a continuous wave in which the most stable and unstable conformations correspond to conformers B ( $\theta = 180^\circ$ ) and A ( $\theta = 0^\circ$ ), respectively. These data clearly show that the formation of an intramolecular H-bond is energetically unfavorable for **1**, and this is a notable characteristic which differentiates **1** from **2**.

#### Experimental Part

(+)-*Chelidone* (**1**) was isolated from *Chelidonium majus* (Papaveraceae) in the usual way and crystallized from MeOH/acetone/Et<sub>2</sub>O soln. by slow evaporation at 4°. M.p. 136°. Anal. calc. for C<sub>20</sub>H<sub>19</sub>NO<sub>5</sub>·H<sub>2</sub>O (371.4): C 64.68, H 5.70, N 3.77; found: C 64.57, H 5.64, N 3.84.

Crystallization from EtOH: m.p. 136°. Anal. found: C 64.64, H 5.70, N 3.98.

Crystallization from MeOH: m.p. 136°. Anal. found: C 64.80, H 5.73, N 3.73.

Crystallization from AcOEt: m.p. 136°. Anal. found: C 64.92, H 5.95, N 3.61.

(±)-*Corynoline* (**2**) was isolated from *Corydalis incisa* (Papaveraceae) in the usual way and crystallized under the same conditions. M.p. 216–217° (from CHCl<sub>3</sub>/MeOH). Anal. calc. for C<sub>21</sub>H<sub>21</sub>NO<sub>5</sub> (367.4): C 68.65, H 5.76, N 3.81; found: C 68.67, H 5.79, N 3.80.

*Crystal-Structure Determination and Refinement.* A single crystal (ca. 0.3 × 0.3 × 0.4 mm) was used for X-ray studies. The crystal data is summarized in Table 3. The unit cell parameters were determined by a least-squares fit of 2 $\theta$  angles for 25 reflections (30° < 2 $\theta$  < 60°). The crystal density was measured by the flotation method using an aq. KI soln. X-Ray diffraction intensities within 2 $\theta$  – 130° were measured at 293 K by a Rigaku AFC-5 diffractometer employing the  $\omega$  – 2 $\theta$  scan technique with a scan speed of 3° min<sup>-1</sup>; the scan width was (1.0 + 0.15 tan $\theta$ )° (in  $\theta$ ) with 3-s backgrounds measured at two extremes of the scan peak. The intensities of 4 standard reflections measured every 100 reflections remained constant to within ±1% of their mean values. The measured intensities were then subjected to Lorentz and polarization corrections. A total of 1561 independent reflections were used for structure determination and refinement.

Table 3. *Crystal Data of 1*

Formula	C <sub>20</sub> H <sub>19</sub> NO <sub>5</sub> ·H <sub>2</sub> O	$V$ [Å <sup>3</sup> ]	869.0(5)
Mol. wt.	371.38	$Z$	2
Crystal system	monoclinic	$d_x$ [g·cm <sup>-3</sup> ]	1.411
Space group	$P2_1$	$d_m$	1.410
$a$ [Å]	8.971(1)	$F(000)$	388
$b$ [Å]	9.120(1)	Radiation	Cu-K $\alpha$
$c$ [Å]	10.640(2)	$\lambda$ [Å]	1.5418
$\beta$ [°]	93.43(3)		

The structure was solved by the direct method with program MULTAN [14], and then refined by the full-matrix least-squares method with isotropic thermal parameters, and then by block-diagonal least squares with anisotropic parameters. The H-atom positions were located from a subsequent difference *Fourier* map. The function minimized was  $\Sigma \omega(|F_o| - |F_c|)^2$ . The weighting scheme used for the least-squares refinement was as follows:  $\omega = 1.43032$  for  $F_o = 0.0$  and  $\omega = 1.0/[\sigma(F_o)^2 + 0.10449|F_o| - 0.00057|F_c|]^2$  for  $F_o > 0.0$ , where  $\sigma(F_o)^2$  is the standard deviation based on counting statistics. The discrepancy indexes  $R$  and  $R_w$  were 0.055 and 0.052, resp.;  $S = [\omega|F_o| - |F_c|]^2/(M - N)^{1/2}$ , where  $M =$  no. of observed reflections and  $N =$  no. of variables) was 1.98. None of the positional parameters shifted more than one fifth from its standard deviation, and maximum electron density in the final *Fourier* synthesis was  $0.34 \text{ e} \cdot \text{Å}^{-3}$ .

For all crystallographic computations, the UNICS programs [15] were used, and atomic scattering factors were from International Tables for X-Ray Crystallography [16]. All numerical calculations were carried out on a *Micro Vax II* computer at the Computation Center of Osaka University of Pharmaceutical Science.

**Thermal Analysis.** Differential thermal analysis and thermogravimetry (DTA-TG) was carried out in air. A standard-type differential scanning calorimeter produced by *Rigaku Denki Co., Ltd.* was used to measure the amount of heat. An aluminium cell was used as a sample (8.82 mg) container and a heating rate of 2.5°/min was adopted. For the calculation of the amount of heat, the heat of transition of KNO<sub>3</sub> and H<sub>2</sub>O was employed as a standard.

**<sup>1</sup>H-NMR Measurements.** <sup>1</sup>H-NMR spectra: *Varian VXR-500* (499.8 MHz) spectrometer; sample concentration ca. 1.00–25.00 mg/ml (3–72 mm); CDCl<sub>3</sub> (99.8% isotopic purity) and (CD<sub>3</sub>)<sub>2</sub>SO (99.96%) as solvents;  $\delta$  in ppm rel. to internal tetramethylsilane (= 0 ppm); error within  $\pm 0.001$  ppm. The temperature dependence of  $\delta(\text{OH})$  was determined by seven measurements at 26–55° for each soln.; the temperature-controlled unit has an error within  $\pm 1^\circ$ .

**Conformational-Energy Calculations.** All energy calculations were carried out with the MNDO program [17] operating on a *Micro VAX II* computer. The atomic coordinates of the conformers were constructed by using the bond lengths and angles obtained by X-ray analyses of **1** and **2** [10].

## REFERENCES

- [1] J. M. Probst, *Ann. Pharm.* **1839**, 29, 113.
- [2] F. von Bruchhausen, H.-W. Bersch, *Chem. Ber.* **1930**, 63, 2520; E. Spath, F. Kuffner, *ibid.* **1931**, 64, 370.
- [3] H.-W. Bersch, *Arch. Pharm. (Weinheim)* **1950**, 283, 36; *ibid.* **1958**, 291, 491.
- [4] R. H. F. Manske, in 'The Alkaloids', Academic Press, New York, 1979, Vol. 17, pp. 493–500; *ibid.*, 1985, Vol. 26, pp. 185–240; T. Kametani, in 'The Chemistry of the Isoquinoline Alkaloids' Hirokawa Publishing Company, Tokyo, 1968, Vol. 1, pp. 213–220; *ibid.*, 1974, Vol. 2, pp. 297–304.
- [5] C.-Y. Chen, D. B. MacLean, *Can. J. Chem.* **1967**, 45, 3001; S. Naruto, S. Arakawa, H. Kaneko, *Tetrahedron Lett.* **1968**, 1705.
- [6] M. Cushman, T.-C. Choong, *Heterocycles* **1980**, 14, 1935.
- [7] N. Takao, K. Iwasa, M. Kamigauchi, M. Sugiura, *Chem. Pharm. Bull. (Tokyo)* **1978**, 26, 1880.
- [8] G. Snatzke, J. Hrubek, Jr. Hruban, L. Hruban, A. Horeau, F. Santavy, *Tetrahedron* **1970**, 26, 5013; N. Takao, M. Kamigauchi, K. Iwasa, N. Morita, *Arch. Pharm. (Weinheim)* **1984**, 317, 223.

- [9] G. A. Cordell, N. R. Farnsworth, *Heterocycles* **1976**, *4*, 393; M. Cushman, T.-C. Choong, J. T. Valko, M. P. Koleček, *J. Org. Chem.* **1980**, *45*, 5067.
- [10] M. Kamigauchi, Y. Noda, N. Takao, T. Ishida, M. Inoue, *Helv. Chim. Acta* **1986**, *69*, 1418.
- [11] N. Takao, M. Kamigauchi, K. Iwasa, K. Tomita, T. Fujiwara, A. Wakahara, *Tetrahedron Lett.* **1974**, 805; *Tetrahedron* **1979**, *35*, 1099.
- [12] N. Takao, N. Bessho, M. Kamigauchi, K. Iwasa, K. Tomita, T. Fujiwara, S. Fujii, *Tetrahedron Lett.* **1979**, 495; N. Takao, N. Morita, M. Kamigauchi, K. Iwasa, K. Tomita, T. Fujiwara, S. Fujii, *Acta Crystallogr., Sect. B* **1981**, *37*, 2043.
- [13] M. Ohnishi, D. W. Urry, *Biochem. Biophys. Res. Commun.* **1969**, *36*, 194; M. A. Khaled, M. M. Long, W. D. Thompson, R. J. Bradley, G. B. Brown, D. W. Urry, *ibid.* **1977**, *76*, 224; L. Zetta, F. Cabassi, *Eur. J. Biochem.* **1982**, *122*, 215.
- [14] P. Main, S. E. Hull, L. Lessinger, G. Germain, J. P. Declercq, M. M. Woolfson, 'MULTAN 78, A System of Computer Programs for the Automatic Solution of Crystal Structures from X-Ray Diffraction Data', Universities of York and Louvain, Belgium, 1978.
- [15] T. Ashida, 'The Universal Crystallographic Computing System-Osaka', Library of Programs, Computing Center, Osaka Univ., 1979.
- [16] J. A. Ibers, W. C. Hamilton, 'International Tables for X-Ray Crystallography', Kynoch Press, Birmingham, 1974, Vol. 4.
- [17] M. J. S. Dewar, W. Thiel, *J. Am. Chem. Soc.* **1977**, *99*, 4899.